Available online at www.sciencedirect.com
SCIENCE DIRECT
ELSEVIER
Journal of the European Ceramic Society 26 (2006) 2923–2929
ECERS
www.elsevier.com/locate/jeurceramsoc

Anelastic spectroscopy for studying O vacancies in perovskites

F. Cordero [a,*], A. Franco [a], V.R. Calderone [b], P. Nanni [b], V. Buscaglia [c]

[a] CNR-ISC Istituto dei Sistemi Complessi, Sezione di Roma, Area della Ricerca di Tor Vergata, Via del Fosso del Cavaliere, 100, I-00133 Roma, Italy
[b] DIChePP (Department of Process and Chemical Engineering), University of Genoa, Fiera del Mare, P.le Kennedy, I-16129 Genoa, Italy
[c] CNR-IENI, Institute for Energetics and Interphases, Department of Genoa, via De Marini 6, I-16149 Genoa, Italy

Available online 10 March 2006

Abstract

We present the results of anelastic relaxation experiments (2–30 kHz) on ceramic $SrTiO_3$ subjected to reduction in H_2 atmosphere, which yield a balance between V_O and $(OH)^-$ defects. The resulting anelastic spectrum contains, besides the well-known structural transformation near 110 K, several thermally activated relaxation processes between 200 and 700 K. The two main elastic energy loss peaks are proposed to provide the first measurement of the hopping rate of V_O –$(OH)^-$ defects in pure $SrTiO_3$.

PACS: 61.72.Ji; 62.40.+i; 66.30.Dn

Keywords: Perovskites; Anelastic spectroscopy

1. Introduction

Oxygen vacancies (V_O) are considered as one of the most common defects in perovskites, and are held responsible for a variety of effects, often undesired, such as fatigue, aging, doping of charge carriers in ferroelectric and dielectric materials; they are also introduced on purpose in order to obtain ionic conduction and are thought to play an important role in determining the physical properties of earth's lower mantle, whose prevalent phase is a perovskite. Yet, the microscopic parameters of V_O in perovskites, such as the activation energy for diffusion, are generally known with great uncertainty. Strontium titanate is an emblematic case; it has been studied for over 50 years as a model system where the quantum paraelectric state prevents ferroelectricity, and superconductivity may be induced by doping,[1] generally with O vacancies; in addition, it is used in various technological applications, notably film substrates and capacitors. The mobility of V_O in $SrTiO_3$, however, is poorly characterized, as demonstrated by a recent compilation of O chemical diffusion data.[2] Even more striking are the recent indications that the V_O introduced by high temperature reduction are not uniformly distributed over the bulk, as generally assumed for both crystals and ceramics, but would form clusters[3] or might form only in highly defective near-surface layers.[4] Such observations put into discussion much of the past research on $SrTiO_3$, especially on polaronic effects, including the belief that it supports a metal-insulator and superconducting transition at very low densities of carriers.

Here, we discuss how the anelastic spectroscopy, namely the measurement of the complex dynamic elastic modulus $M = M' + iM''$ or compliance $s = s' - is'' = M^{-1}$, may significantly contribute to the study of the mobility and ordering of V_O in perovskites. In fact, a V_O has a quadrupolar symmetry that is in principle associated with a tetragonal strain reorienting by 90° after each jump (see Fig. 1), whereas the associated electric dipole is null in a perfect cubic perovskite. Then, the dynamic compliance at frequency ω provides a direct measure of the hopping rate τ^{-1} through the condition $\omega\tau = 1$ at the absorption maximum, exactly like for dielectric spectroscopy, but without the contribution of free charges to the relaxation spectrum.

After introducing an interpretative framework and reviewing the few existing data in the literature, preliminary results will be presented on the hopping dynamics of V_O in $SrTiO_3$ reduced in H_2 atmosphere.

2. Anelastic and dielectric relaxation from O vacancy hopping

An O vacancy in a cubic perovskite ABO_3 has tetragonal symmetry, with quaternary axis along the direction of the nearest

* Corresponding author. Tel.: +39 06 4993 4114; fax: +39 06 4993 4663.
E-mail address: francesco.cordero@isc.cnr.it (F. Cordero).

0955-2219/$ – see front matter © 2006 Elsevier Ltd. All rights reserved.
doi:10.1016/j.jeurceramsoc.2006.02.008

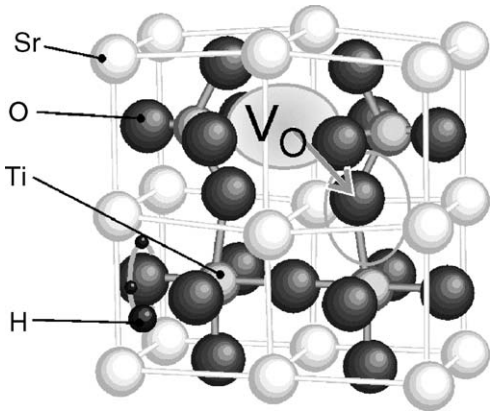

Fig. 1. O vacancy with the ellipsoid representing the anisotropic elastic dipole λ; the jump indicated by the arrow reorients λ by 90°. Also, indicated is the ring of four positions of H around a Ti—O bond.

neighbour B atoms, as shown in Fig. 1. Therefore, a uniform concentration c_x of V_O with tetragonal axis x will give rise to an anisotropic strain

$$\varepsilon = c_x \begin{bmatrix} \lambda_1 & 0 & 0 \\ 0 & \lambda_2 & 0 \\ 0 & 0 & \lambda 2 \end{bmatrix} = c_x \lambda^{(x)} \tag{1}$$

and similarly for the other orientations $\alpha = y, z$, where $\lambda^{(\alpha)}$ is called elastic dipole tensor,[5] by analogy with the electric and magnetic dipole, although it is actually a quadrupole. The uniaxial strains along the tetragonal axis, λ_1, and in the perpendicular plane, λ_2, are negative in case of compression and positive in case of expansion. Fluctuations in the populations c_α of the three types of orientations are reflected as strain fluctuations, since $\varepsilon = \Sigma_\alpha c_\alpha \lambda^{(\alpha)}$; for the cubic case, the fluctuating symmetric strains are of tetragonal symmetry, $\varepsilon^{\mathrm{t}} = 2\varepsilon_3 - \varepsilon_1 - \varepsilon_2$, and orthorhombic symmetry, $\varepsilon^{\mathrm{o}} = \varepsilon_1 - \varepsilon_2$ (using the notation $\varepsilon_1 = \varepsilon_{xx}$, etc.). The tetragonal strain is coupled to fluctuations of the type $c_z = c/3 + \delta c$ and $c_{x,y} = c/3 - \delta c/2$, giving rise to $\varepsilon^{\mathrm{t}} = 2\delta c(\lambda_1 - \lambda_2)$, and similarly for the orthorhombic strain; clearly, the strain fluctuations are proportional to the anisotropic component $\Delta\lambda = \lambda_1 - \lambda_2$ of the elastic dipole. Both strains are related to the corresponding stresses through the elastic compliance $s_{11} - s_{12}$, as $\varepsilon^{\mathrm{t,o}} = (s_{11} - s_{12})\,\sigma^{\mathrm{t,o}}$. The application of a periodic stress σ with angular frequency ω perturbs the elastic energies of the various dipoles and therefore their populations, resulting in a strain response out of phase of ϕ with respect to stress; then, the compliance acquires a complex relaxational component[5]

$$\delta(s_{11} - s_{12}) = \frac{2}{3}\frac{cv_0}{k_{\mathrm{B}}T}(\Delta\lambda)^2 \frac{1}{1 + i\omega\tau} \tag{2}$$

where τ is the relaxation time, related to the hopping rate Γ of a V_O to a specific nearest neighbour position through $\tau^{-1} = 12\Gamma$. The imaginary part produces absorption, and the elastic energy loss coefficient, or reciprocal of the mechanical Q, is $Q^{-1} = \tan\phi = s''/s'$ or, neglecting the relaxational contribution to s' and setting $s' = s_{11} - s_{12}$,

$$Q^{-1} = \frac{2}{3}\frac{cv_0(\Delta\lambda)^2}{(s_{11} - s_{12})k_{\mathrm{B}}T}\frac{\omega\tau}{1 + (\omega\tau)^2} \tag{3}$$

which is peaked at $\omega\tau = 1$. Measurements are generally made as a function of temperature at the fixed frequencies determined by the sample or transducer resonances. The factor 2/3 in the above equation is valid for application of $\sigma^{\mathrm{t,o}}$ stresses to a single crystal; for a polycrystal, it should be reduced due to angular averaging and porosity. Note that the dielectric relaxation is given by the same expressions with electric dipoles **p** instead of elastic quadrupoles λ, dielectric susceptibility χ instead of the compliance s and possibly slightly different factors relating the relaxation time to the hopping rates.[6] When interpreting dielectric experiments, it is customary to neglect the temperature dependence of the relaxation strength, which is simply set to $(\varepsilon_0 - \varepsilon_\infty)/\varepsilon_\infty$.

To our knowledge, no measurements of the elastic quadrupole tensor λ of V_O in perovskites exist, but first principle calculations indicate small atomic displacements around an V_O in $SrTiO_3$ and $PbTiO_3$, mainly determined by the electrostatic interactions between the ions, and almost negligible and isotropic long range distortions,[7] although more recent calculations on larger supercells indicates more substantial displacements[8,9]; the exaggerated cation displacements in Fig. 1 are based on these works. It is therefore possible that the anisotropic component $\Delta\lambda = \lambda_1 - \lambda_2$ and therefore the amplitude of the anelastic relaxation due to V_O hopping are rather small. Yet, V_O hopping in a perovskite is in principle detectable by anelastic relaxation, while it is not by dielectric relaxation. In fact, there is no electric dipole associated with a V_O, unless some chemical disorder exists; for example, if a V_O is trapped at a Fe^{3+} substituting a Ti^{4+} in $SrTiO_3$, then an electric dipole is created within the Ti^{4+}–V_O–Fe^{3+} cluster. In this case, however, one measures the hopping rate around the dopant and not in the regular lattice.

2.1. Jumps between inequivalent sites

If for simplicity, we consider a small amount of acceptor dopants in the B sublattice of ABO_3 inducing the formation of V_O, e.g. Fe_{Ti}, the potential profile for V_O hopping should appear as in Fig. 2. Hopping between O sites far from the dopants occurs over a barrier E_f with a mean rate Γ_f, while hopping around the dopants occurs over a barrier E_t with a mean rate Γ_t; also indicated in the figure is the binding energy E_b of the complex dopant-V_O. Jumps of the type $3 \rightarrow 2$ for the vacancy

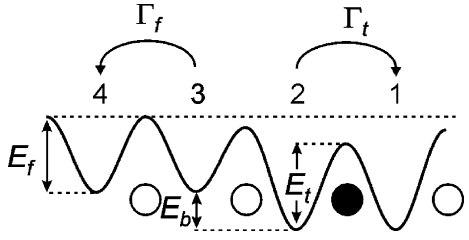

Fig. 2. Potential energy profile felt by an O vacancy hopping near a trapping donor impurity (black circle).

to get trapped and the reverse jumps may occur at two different rates, depending on the saddle points between 2–3 and 1–2. We are not aware of any systematic attempt at evaluating the effect of dopants on the potential energy for V_O hopping, but it may be non-trivial; for example, it has been found that the reorientation barriers of the dopant-V_O complex in $CaTiO_3$ and $KTaO_3$ are as low as 0.1–0.4 eV[10] and 0.25–0.3 eV for Mg_{Ti}–V_O in $SrTiO_3$,[11] while more typical values for the V_O hopping barriers in Ti-based perovskites seem to be 1 Ev.[12–17] According to this analysis, one might expect to observe a spectrum of anelastic and dielectric peaks like Eq. (3), with different peaks corresponding to the various types of jumps. These peaks may have large differences in the intensities, so that some of them are unobservable, and may be largely distorted in shape with respect to Eq. (3), which is valid for relaxation between states of the same energy. It can be shown[18] that a relaxation mode involving two states differing in energy by $E_1 - E_2 = \Delta E$ has an intensity proportional to $n_1 n_2/T$ (in the high dilution limit of defects), where n_1 and n_2 are the populations of the two states. For $\Delta E/k_B T \to 0$, this depopulation factor approaches $1/T$, as in Eq. (3), but it reduces the relaxation intensity when $k_B T < \Delta E$, finally becoming proportional to $\exp(-\Delta E/k_B T)$. In the case of only two possible states it is:

$$\frac{n_1 n_2}{T} = \frac{1}{T \cosh^2(\Delta E/2k_B T)} \quad (4)$$

which presents a maximum at $k_B T = 0.65E$. The physical origin for this factor is that the anelastic or dielectric relaxation results from changes in the defect populations induced by the applied field, and therefore states that are little populated (because $\Delta E > k_B T$) contribute little to relaxation. This fact is generally overlooked, but it may render unobservable relaxation processes between states differing in energy by few tenths of eV, or distort the shape of the corresponding relaxation peaks, due to the factor $\exp(-\Delta E/k_B T)$, so changing the apparent activation energy. Also the relaxation time is affected, in the case of relaxation between two states being multiplied by $\cosh(\Delta E/2k_B T)$, but this effect is less important in determining the peak position and shape. Therefore, in the presence of dopant impurities or in solid solutions where disorder in the site energies is expected, the simple evaluation of the hopping barrier for V_O from the condition $\omega\tau(T_p) = 1$ for the peak temperature combined with the Arrhenius law $\tau = \tau_0(E/k_B T)$ might give erroneous results and the whole peak should be analyzed as a function of frequency and temperature.

3. Existing anelastic experiments on O vacancies in perovskites

Studies of the mobility of V_O by anelastic experiments have been reported in few oxide-ion conductors. Notably, in Y stabilized zirconia (YSZ, not a perovskite), a thorough series of combined dielectric, anelastic, tracer diffusion and electrical conductivity experiments has been carried out ([19] and references therein), finding several effects, like differences in the activation enthalpies associated with the electrical conduction, diffusion and reorientation processes, and trapping and clustering of the V_O. Clear anelastic and dielectric relaxation peaks with $E \approx 1$ eV and $\tau_0 \sim 10^{-16}$–10^{-14} s, and attributed to V_O hopping, have also been found in $La_2Mo_2O_9$, which again is not a perovskite.[20] Interestingly, it is observed that the dielectric relaxation strength does not follow the expected $1/T$ dependence but is almost constant between 500 and 800 K; we may speculate that this is due to disorder in the site energies with $\Delta E/k_B \sim 1000$ K, which makes the relaxation strength of the type of Eq. (4) almost stationary in that temperature range. In perovskites, an anelastic relaxation process with $E \approx 1$ eV is found in PZT,[21,22] where however the spectrum is complicated by the motion of ferroelectric domain walls. The peak presents a different shape and temperature position when measured on heating and on cooling, but its intensity varies as expected from hopping of V_O, if their concentration is modified by annealing in vacuum or in O_2 [21]; instead, the peak intensity is depressed by both doping with Nb and K, which should, respectively, inhibit and promote the presence of V_O[22]. Recent work has focused on the role that V_O plays in the ferroelectric fatigue of $Bi_4Ti_3O_{12}$ (BiT), by measurement of the anelastic spectra.[23,24] Again, the situation is complicated, since V_O hopping has been associated with both a dielectric relaxation, having $E = 0.7$ eV, and the accompanying anelastic peak[24] and to a dielectric relaxation with $E = 1.9$ eV whose anelastic counterpart seems to be a peak with $E = 1.5$ eV[23]; it should also be noted that in the Aurivillius structure of BiT the V_O should be mostly found in the BiO layers rather than in the perovskite blocks, and there are additional relaxation processes related to ferroelectric domain wall motion.[23] Finally, the case of Yb-doped $SrZrO_3$ and $SrCeO_3$ should be mentioned; after a treatment in wet atmosphere to obtain proton conduction, complex anelastic spectra are found, where a peak with $E = 0.8$ eV is attributed to reorientation of the Yb–V_O complex.[25] Strontium titanate is in principle a perfect system for identifying the anelastic relaxation process due to V_O hopping for various reasons: (i) it remains cubic down to $T_C = 105$ K, and is therefore free from domain walls; (ii) it is reported to support large amounts of V_O after reducing treatments, this type of doping having been used even for inducing superconductivity[1]; (iii) as mentioned in the introduction, it has been studying for over 50 years but a detailed revisitation of the role of V_O is occurring.

4. Experimental and results

Ceramic samples were prepared by solid-state reaction of $SrCO_3$ (Aldrich, 99.9%) and TiO_2 (Aldrich, 99.9%) mixtures for 6 h at 1100 °C. The resulting powder was milled, sieved and pressed in parallelepipeds about 45 mm × 10 mm × 10 mm, which were sintered in air at 1450 °C. The resulting ceramics showed homogeneous microstructure and a relative density of 97%. Bars were cut and polished to dimensions 45 mm × 5 mm × 0.5 mm, suitable for the measurements of the dynamic Young's modulus, $M(\omega,T) = M' + iM''$; the dynamic compliance $s(\omega,T) = M^{-1}(\omega,T)$ contains a combination of all the s_{ij} components, due to the polycrystalline nature of the samples. The complex modulus was measured by electrostatically exciting the flexural modes of the sample, which was suspended with thin thermocouple wires at the nodal lines. The resonance frequencies $\omega_n/2\pi$ are in the ratio 1:13.2 for the first and fifth

flexural modes,[5] which we generally excite during the same measurement run, since they have nearly coincident nodal lines. The temperature variation of the real part M' can be deduced from that of the resonance frequencies, since $\omega_n = \alpha_n h/l^2(M'/\rho)^{1/2}$, where h, l and ρ are the sample thickness, length and density, which generally vary with temperature much less than M', and α_n is a geometrical factor for the nth mode. Therefore, one can assume $M'(T)/M(T_0) = \omega^2(T)/\omega^2(T_0)$, where T_0 is any reference temperature (in the figures below we chose the temperature where $M'(T)$ is maximum). The elastic energy loss coefficient is $Q^{-1} = M''/M' = s''/s'$ and, according to Eqs. (3) and (4), the hopping or reorientation of defects with a rate τ^{-1} between states differing in energy by ΔE and separated by a mean barrier E produces a peak in Q^{-1} of the form

$$Q^{-1} \propto \frac{(\Delta\lambda)^2}{T\cosh^2(\Delta E/2k_BT)} \frac{\alpha(\omega\tau)^\alpha}{1+(\omega\tau)^{2\alpha}} \quad (5)$$

with $\tau = \tau_0(E/k_BT)/\cosh(\Delta E/2k_BT)$, where the Fuoss–Kirkwood parameter $\alpha < 1$ reproduces a possible peak broadening with respect to the pure Debye case. The Fuoss–Kirkwood distribution of relaxation times[5] produces the frequency dependence of the imaginary susceptibility as in Eq. (5) and is popular for analyzing anelastic data; the peak shape is slightly different from that obtained from other expressions, like the Cole–Cole one generally preferred in the literature on dielectric spectroscopy, but there are no physical grounds for preferring one over the other. Fig. 3 presents Q^{-1} and the real part of the Young's modulus M normalized to its maximum value before (thin line) and after (empty symbols) a reduction treatment of a sample wrapped in Zr foil and heated at 1000 °C for 3 h in a vacuum of $<10^{-8}$ mbar. A sharp increase of $Q^{-1}(T)$ and a drop of $M'(T)$ occur at the cubic-to-tetragonal transformation at $T_C = 110$ K. The transformation temperature T_C has been reported to vary with the level of electron doping n as $dT_C/dn = -2400$ K/mol[26] or -1800 K/mol[27] in $SrTiO_{3-\delta}$ reduced in H_2; assuming $n = 2$, it should provide a measure of δ, even though it depends on several other factors, including near-surface strains that may cause a gradient in T_C.[28] After the reduction treatment in vacuum with

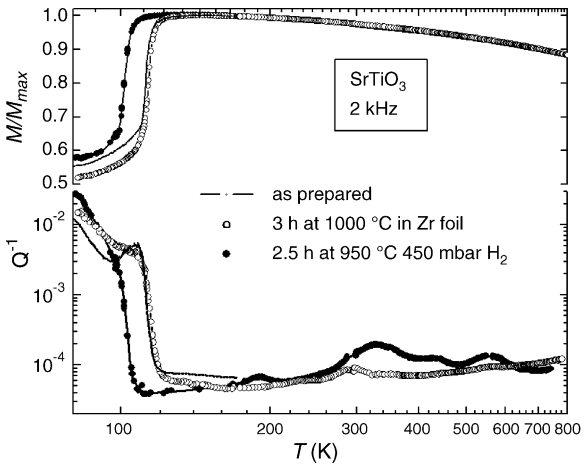

Fig. 3. Elastic energy loss Q^{-1} and relative variation of the Young's modulus (M/M_0-1) of $SrTiO_3$ measured at $\omega/2\pi = 2$ kHz in the as prepared state and after two different reduction treatments.

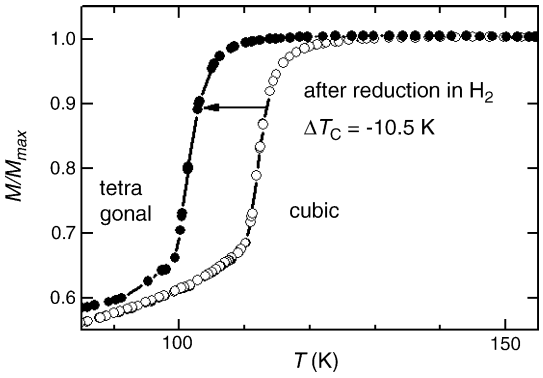

Fig. 4. Young's modulus around the cubic-to-tetragonal transition before (open symbols) and after (closed symbols) the reduction treatment in H_2 atmosphere.

Zr foil, the sample colour and T_C were almost unchanged and the high temperature spectrum remained flat; we conclude that no appreciable O loss occurred.

In order to further reduce the O_2 partial pressure through the equilibrium reaction $H_2 + \frac{1}{2}O_2 \leftrightarrow H_2O$, we treated a sample in 450 mbar of H_2 at 950 °C for 3 h. At 950 °C, it is $p_{O_2} = 4 \times 10^{-15}$ mbar $\times (p_{H_2O}/p_{H_2})^2$, but we could not measure the actual partial pressures in the sample chamber; the treatment was done in a quartz tube connected to a UHV system and a flux of H_2 was maintained in order to remove the H_2O produced by the reaction with the O_2 evolved from the sample. The sample changed colour from white-yellow to uniform dark grey and exhibited metallic conductivity at room temperature; the filled symbols in Fig. 3 show that T_C was now shifted to lower temperature and new peaks appeared in the $Q^{-1}(T)$ curve.

Fig. 4 presents the elastic modulus $M'(T)$ around T_C. The determination of the exact value of T_C from the $M'(T)$ curves requires the separation of the intrinsic softening and critical attenuation due to the structural phase transformation from those due to the motion of domain walls immediately below T_C; it is clear, however, that the reduction treatment produced a shift of the step in the modulus of $T_C = -10.5$ K, which, assuming $\delta = 0$ initially, $n = 2\delta$ after the treatment, and $dT_C/dn = -2100$ K/mol averaging the results of Refs.,[26,27] yields $\delta \approx 0.0025$. We consider this estimate only indicative, since it neglects the possible occurrence of H intake, and we think that the reduction treatment introduced H defects, especially in view of the relatively low temperature and high H_2 pressure at which it was performed. We do not know whether H contributes to the negative shift of T_C through additional electron doping or not, since the effects of different types of doping on T_C are not obvious; for example, partially substituting Ti^{4+} with Nb^{5+} rises T_C instead of lowering it.[26]

5. Discussion

We are not aware of any direct measurement of the hopping rate of V_O in $SrTiO_3$ not containing cation dopants, but there are several indications that the hopping barrier E_f (see Fig. 2) should be close to 1 eV, as for other titanate perovskites.[17] The activation energy for O tracer diffusion was determined through isotope exchange as $E = 1.1$ eV between 850 and 1350 °C in

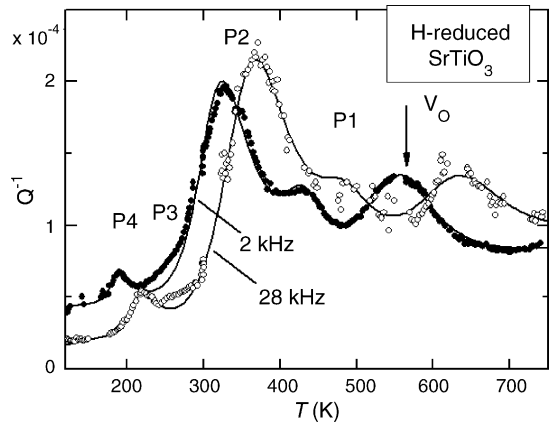

Fig. 5. Anelastic spectrum of $SrTiO_3$ after reduction in H_2, measured at two frequencies. The continuous line is a fit as described in the text. The arrow at 566 K signals where a peak at $\omega/2\pi = 2$ kHz is expected, if the O vacancies jump over a barrier $E = 1$ eV.

annealed crystals,[12] while values as low as 0.67 eV in unannealed crystals were attributed to faster diffusion along dislocations. Electrical conductivity experiments in $SrTiO_3$ doped in different manners indicate an activation energy for the V_O mobility $E = 0.86$ eV.[15] Direct measurements of the reorientation rate of V_O around the dopant may be obtained from dielectric spectroscopy, and in $Sr_{1-1.5x}Bi_xTiO_3$, it is found $E_t = 1$–1.1 eV,[16] while a dielectric relaxation process in $SrTi_{1-x}(Mg_{1/3}Nb_{2/3})_xO_3$ with $E_t = 0.25$–0.3 eV is attributed to a V_O reorienting around a Mg dopant[11]; the latter results demonstrate that the influence of dopants on the potential for V_O hopping may be substantial.

As discussed above, we expect that the anelastic spectrum of reduced $SrTiO_3$ contains a peak due to V_O hopping in the unperturbed lattice; in fact, unlike dielectric spectroscopy, binding to a dopant or defect in order to produce an electric dipole is not necessary. For point defects, it is $\tau_0 \sim 10^{-13}$ s and therefore we expect that V_O hopping with $E_f = 1$ eV gives rise to a peak around 566 K for $\omega/2\pi = 2$ kHz. Fig. 5 presents the $Q^{-1}(\omega,T)$ curves at $\omega/2\pi \sim 2$ kHz and 28 kHz, and the peak labelled V_O is exactly at that temperature (indicated by an arrow); we therefore assign it to V_O hopping. However, several other peaks appear after the reduction treatment in H_2, and it is likely that some of them are due to H related defects. The whole spectrum has been fitted with four processes of the form of Eq. (5), as shown by the continuous lines in Fig. 5, with the parameters reported in Table 1; the comparison between fit and data evidences the presence of an additional peak labelled P3.

All the peaks except P4 have a relaxation rate with $\tau_0 = 10^{-14}$–10^{-13} s, which is compatible with point defect hopping or reorientation; instead, the larger value of τ_0 of P4 suggests a collective type of motion. All the processes except P4 are considerably broader than pure Debye relaxations, as indicated by the low values of α; the intensity of P2 increases with temperature, and this is reproduced in terms of relaxation between states differing in energy by $\Delta E \sim 0.08$ eV.

Table 1
Experimental data for Fig. 5

	E (eV)	ΔE (eV)	τ_0 (s)	α
V_O	0.98	0	1×10^{-13}	0.7
P1	0.85	0	1×10^{-14}	0.76
P2	0.61	0.08	2×10^{-14}	0.5
P4	0	0	2×10^{-12}	1

Peak V_O has two unexpected features. One is that it is present already in the as-prepared state, with an intensity about 5.5 times smaller than after the reduction treatment in H_2, as shown in Fig. 6. If we accept the estimate from $\Delta T_C = -10.5$ K that the reduction increased the content of V_O by $\Delta\delta \sim 0.0025$, and assume the intensity of peak V_O increases linearly with δ, then we obtain $\delta_0 \sim 5 \times 10^{-4}$ in the as prepared state and $\delta \sim 0.0028$ after reduction. The value of δ_0 is perfectly compatible with a small, unwanted, off-stoichiometry in sample preparation, for example Sr vacancies, or to the presence of acceptor impurities which are electrically compensated by V_O. We cannot exclude that the compensating V_O bound to these unwanted defects give rise to a small thermally activated peak that we generally observe around room temperature, and also appears in the curve with open symbols in Fig. 3. In this case, the residual peak V_O would be due to the fraction of such O vacancies that are detrapped from the impurities, so explaining why the peak V_O does not shift after the introduction of additional free vacancies.

The other interesting feature of peak V_O is its width, quantified in the value $\alpha = 0.7$ of the Fuoss–Kirkwood parameter; the curve corresponding to monodispersive relaxation with $\alpha = 1$ and all the other parameters unchanged, is shown with a dashed line in Fig. 6. There are two main categories of peak broadening in crystalline solids: inhomogeneous broadening due to interaction with a distribution of static impurities and distortion of the peak shape due to interaction of the relaxing defects among themselves. In the first case, the broadening is mostly due to a distribution of energy barriers, while the distribution of τ_0

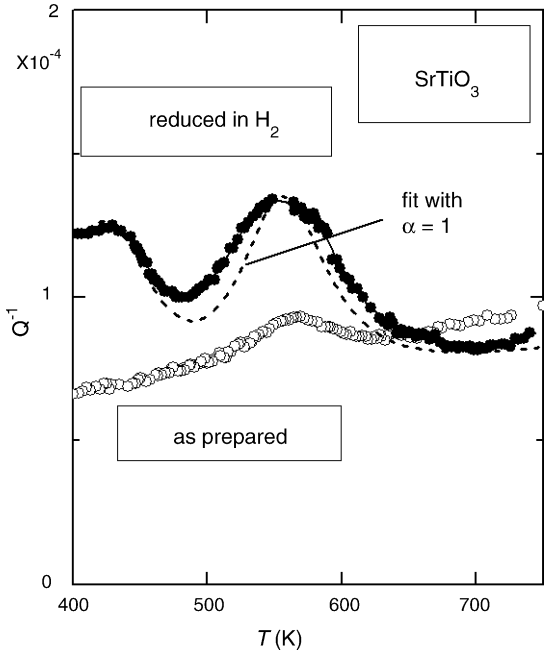

Fig. 6. Peak V_O measured at 2 kHz in the as-prepared and reduced state. The dashed line corresponds to the absence of peak broadening ($\alpha = 1$).

can usually be neglected; the Fuoss–Kirkwood distribution of relaxation times,[5] which integrated over ln τ gives rise to the dispersion in Eq. (5), is

$$g_{FK}(\alpha, x) = \frac{2}{\pi} \frac{\cosh(\alpha x)\cos(\alpha\pi/2)}{\cos^2(\alpha\pi/2) + \sinh^2(\alpha x)} \quad (6)$$

where $x = \ln(\tau/\tau_{max})$ and τ_{max} is the mean relaxation time at the peak temperature; $g_{FK}(0.7,x)$ may be approximated as a Lorentzian with full width at half maximum $w \sim 1.44$. Since $\ln \tau = \ln \tau_0 + E/k_B T$, the corresponding distribution of activation energies is again a Lorentzian with temperature dependent width $w_E/k_B = 1.44 \times T \sim 850$ K, which seems too large for a crystalline system with a concentration of defects of the order of 10^{-3} mol, at least when compared with metallic systems where the random energy shifts are due to strain interactions. For example, the peak due to hopping of interstitial O in Nb is monodispersive for 0.1 at% O and remains narrower than peak V_O up to 1 at% O,[29] the broadening being due to elastic interactions among the elastic quadrupoles associated with the O defects. Even taking into account the electrostatic interaction among the V_O^{2-} at an average distance of five lattice constants and with a dielectric constant >100, it is difficult to imagine fluctuations of the electrostatic energies sufficient to explain the width of peak V_O. The explanation in terms of inhomogeneous broadening would then require that V_O hopping occurs in a highly defective environment, which produces random shifts in the site and barrier energies of the order of $E/k_B \sim 800$ K. This would be in agreement with the recent assertion that V_O in $SrTiO_3$ are confined to highly defective surface layers.[4] The surface strains, whether due to dislocations[3,4] or to surface effects in the otherwise perfect crystallites,[28,30] may extend far below the crystallite surface, up to tens of microns in perfect single crystals,[30] a distance much larger than the average grain size in our samples. In both cases, if the observations reported for large crystals are valid also for the grains in the ceramic, one concludes that these grains must be highly strained. Such strains are reported to rise the temperature of the cubic-to-tetragonal instability of tens of Kelvin,[28,31] and this might be the reason why the $M(T)$ curve of the as-prepared sample (Fig. 4) indicates $T_C \sim 110$ K, while it is generally reported $T_C = 105$ K in single crystals. Another source of deviation from Debye relaxation is the homogeneous interaction among the V_O elastic dipoles, which can be treated in mean-field approximation[32,33] and yields an enhancement of the relaxation time τ and strength Δ by a Curie–Weiss-like factor $(1 - T_0/T)^{-1}$, where T_0 is the temperature at which the elastic dipoles start ordering parallel to one of the possible directions due to elastic interaction. Such a temperature is proportional to the strength of interaction among the dipoles,[34] $T_0 \propto c(\Delta\lambda)^2$ and is therefore also proportional to the intensity of the peak due to the hopping/reorientation of the elastic dipoles, Eq. (3). In this manner, even if in the present case neither $c = \delta$ nor $\Delta\lambda$ are known and the peak shape could be reliably measured only at the lowest frequency, it is possible to assess whether strain induced ordering of the V_O may play a role in inducing noticeable changes in the peak shape. The comparison can be made with the anelastic relaxation process due to hopping of V_O in the RuO_2 planes of the ruthenocuprate superconductor $RuSr_2GdCu_2O_{8-\delta}$,[35] which correspond to the BO_2 planes in the perovskite structure. In $RuSr_2GdCu_2O_{8-\delta}$, a concentration $\delta \sim 0.02$–0.03 of V_O produced a peak with intensity $Q^{-1}_{max} = 0.011$, therefore 200 times more intense than peak V_O in $SrTiO_{3-\delta}$ of Fig. 6, where $Q^{-1}_{max} = 5 \times 10^{-5}$. Since peak intensity Q^{-1}_{max} and interaction strength or ordering temperature T_0 are both proportional to $c(\Delta\lambda)^2$ through quantities like elastic compliances and molecular volume, which do not vary too much from $RuSr_2GdCu_2O_8$ to $SrTiO_3$, it can be concluded that the interaction strength connected with peak V_O in $SrTiO_3$ is about 200 times smaller than for the peak found in $RuSr_2GdCu_2O_8$.[35] Therefore, strain induced ordering cannot be the cause of the deviation of peak V_O from Debye behaviour, unless the dipoles were confined in regions with much higher than the average value, so that the value of c entering in $T_0 \propto c(\Delta\lambda)^2$ is the large local concentration, whereas that entering in the peak intensity $Q^{-1}_{max} \propto c v_0 (\Delta\lambda)^2$ is the small averaged over all the sample volume. This situation would be met both in the case that V_O are confined near the surface[4] or are aggregated into clusters[3]; however, especially in view of the poor quality of the data at higher frequency, it is not yet possible to come to a definitive conclusion on the nature of the broadening of peak V_O and hence on the possible clustering or confinement of the V_O in $SrTiO_3$.

The peaks at lower temperature are likely to be due to H defects introduced by the reduction in H_2 atmosphere and possibly to polarons connected with both V_O and hydrogen. Anelastic relaxation peaks with $E \sim 0.6$ eV have indeed been observed in proton conducting perovskite cerates[25,36] doped in order to have compensating V_O later filled with $(OH)^-$ ions through exposure to humid atmosphere. A variety of dielectric relaxation peaks have also been found in Bi-doped $SrTiO_3$, one of which is comparable to P1 in Fig. 5 and has been attributed to some polaronic mechanism.[16]

6. Conclusions

Our present knowledge on the formation, mobility and ordering or clustering of O vacancies in perovskites is still confused, even in a classical system like $SrTiO_3$. Anelastic spectroscopy is in principle an ideal tool for investigating these issues, since the anisotropic quadrupolar strain field of an O vacancy is coupled to stress also in the perfect perovskite lattice, whereas the dielectric spectroscopy is only sensitive to hopping of vacancies associated with a defect producing an electric dipole. We chose $SrTiO_3$ as the starting point of our investigation, since it remains cubic in the temperature range of interest and in consideration of the recent findings of non-homogeneous distribution of O vacancies even in pure crystals. In these preliminary experiments, it was not possible to introduce a sufficiently high concentration of O vacancies without the complication of additional H defects, so obtaining a complicated anelastic spectrum. Still, an elastic energy loss peak is found with an activation energy of 1 eV, which most likely constitutes the first direct measurement of the hopping rate of O vacancies in pure $SrTiO_3$. The considerable peak width supports the view that a large fraction of O vacancies are confined within a highly defective surface layer in $SrTiO_3$ crystals or that O vacancies are clustered.

Acknowledgements

This work was done within the programme between CNR and MIUR – FISR DM. 17/12/2002 (and the COST Action 525).

References

1. Schooley, J. F., Hosler, W. R. and Cohen, M. L., Superconductivity in semiconducting $SrTiO_3$. *Phys. Rev. Lett.*, 1964, **12**, 474–475.
2. Pasierb, P., Komornicki, S. and Rekas, M., Comparison of the chemical diffusion of undoped and Nb-doped $SrTiO_3$. *J. Phys. Chem. Sol.*, 1999, **60**, 1835–1844.
3. Scott, J. F., Jiang, A. Q., Redfern, S. A. T., Zhang, M. and Dawber, M., Infrared spectra and second-harmonic generation in barium strontium titanate and lead zirconate-titanate thin films: Polaron artifacts. *J. Appl. Phys.*, 2003, **94**, 3333–3344.
4. Szot, K., Speier, W., Carius, R., Zastrow, U. and Beyer, W., Localized metallic conductivity and self-healing during thermal reduction of $SrTiO_3$. *Phys. Rev. Lett.*, 2002, **88**, 75508-1-4.
5. Nowick, A. S. and Berry, B. S., *Anelastic Relaxation in Crystalline Solids*. Academic Press, New York, 1972.
6. Nowick, A. S. and Heller, W. R., Dielectric and anelastic relaxation of crystals containing point defects. *Adv. Phys.*, 1965, **14**, 101–166.
7. Tanaka, T., Matsunaga, K., Ikuhara, Y. and Yamamoto, T., First-principles study on structures and energetics of intrinsic vacancies in $SrTiO_3$. *Phys. Rev. B*, 2003, **68**, 205213-1-8.
8. Buban, J. P., Iddir, H. and Ögüt, S., Structural and electronic properties of oxygen vacancies in cubic and antiferrodistortive phases of $SrTiO_3$. *Phys. Rev. B*, 2004, **69**, 180102-1-4.
9. Luo, W., Duan, W., Louie, S. G. and Cohen, M. L., Structural and electronic properties of n-doped and p-doped $SrTiO_3$. *Phys. Rev. B*, 2004, **70**, 214109-1-8.
10. Nowick, A. S., Fu, S. Q., Lee, W. K., Lin, B. S. and Scherban, T., Dielectric relaxation of paired defects in perovskite-type oxides. *Mater. Sci. Eng. B*, 1994, **23**, 19–24.
11. Lemanov, V. V., Dielectric relaxation in doped $SrTiO_3$ in the regimes of classical thermal activation and of quantum tunneling. *Ferroelectrics*, 2005, **318**, 121–131.
12. Paladino, A. E., Rubin, L. G. and Waugh, J. S., Oxygen diffusion in single crystal $SrTiO_3$. *J. Phys. Chem. Sol.*, 1965, **26**, 391–397.
13. Lohkamper, R., Neumann, H. and Arlt, G., Internal bias in acceptor-doped $BaTiO_3$ ceramics: Numerical evaluation of increase and decrease. *J. Appl. Phys.*, 1990, **68**, 4220–4224.
14. Zafar, S., Jones, R. E., Jiang, B., White, B., Chu, P., Taylor, D. and Gillespie, S., Oxygen vacancy mobility determined from current measurements in thin $Ba_{0.5}Sr_{0.5}TiO_3$ films. *Appl. Phys. Lett.*, 1998, **73**, 175–177.
15. Claus, J., Leonhardt, M. and Maier, J., Tracer diffusion and chemical diffusion of oxygen in acceptor doped $SrTiO_3$. *J. Phys. Chem. Sol.*, 2000, **61**, 1199–1207.
16. Ang, C., Yu, Z. and Cross, L. E., Oxygen-vacancy-related low-frequency dielectric relaxation and electrical conduction in Bi: $SrTiO_3$. *Phys. Rev. B*, 2000, **62**, 228–236.
17. Wang, R.-V. and McIntyre, P. C., *J. Appl. Phys.*, 2005, **97**, 23508-1-8.
18. Cordero, F., Anelastic (dielectric) relaxation of point defects at any concentration, with blocking effects and formation of complexes. *Phys. Rev. B*, 1993, **47**, 7674–7685.
19. Weller, M., Herzog, R., Kilo, M., Borchardt, G., Weber, S. and Scherrer, S., Oxygen mobility in yttria-doped zirconia studied by internal friction, electrical conductivity and tracer diffusion experiments. *Solid State Ion*, 2004, **175**, 409–413.
20. Wang, X. P. and Fang, Q. F., Mechanical and dielectric relaxation studies on the mechanism of oxygen ion diffusion in $La_2Mo_2O_9$. *Phys. Rev. B*, 2002, **65**, 64304-1-6.
21. Wang, Can, Fang, Q. F., Shi, Yun and Zhu, Z. G., Internal friction study on oxygen vacancies and domain walls in $Pb(Zr,Ti)O_3$ ceramics. *Mater. Res. Bull.*, 2001, **36**, 2657–2665.
22. Bouzid, A., Gabbay, M. and Fantozzi, G., Contribution to the comprehension of dissipation phenomena in lead zirconate titanate: aliovalent doping effect. *Mater. Sci. Eng. A*, 2004, **370**, 123–126.
23. Jimènez, B., Jimènez, R., Castro, A., Millàn, P. and Pardo, L., Dielectric and mechanoelastic relaxations due to point defects in layered bismuth titanate ceramics. *J. Phys.: Condens. Matter*, 2001, **13**, 4326–7315.
24. Li, W., Wang, C. J., Zhu, J. S. and Wang, Y. N., Correlation among oxygen vacancies and its effect on fatigue in neodymium-modified bismuth titanate ceramics. *J. Phys.: Condens. Matter*, 2004, **16**, 9201–9208.
25. Zimmermann, L., Bohn, H. G., Schilling, W. and Syskakis, E., Mechanical relaxation measurements in the protonic conductors $SrCeO_3$ and $SrZrO_3$. *Solid State Ionics*, 1995, **77**, 163–166.
26. Bäuerle, D. and Rehwald, W., Structural phase transitions in semiconducting $SrTiO_3$. *Solid State Commun.*, 1978, **27**, 1343–1346.
27. Hastings, J. B., Shapiro, S. M. and Frazer, B. C., Central-peak enhancement in hydrogen-reduced $SrTiO_3$. *Phys. Rev. Lett.*, 1978, **40**, 237–239.
28. Osterman, D. P., Mohanty, K. and Axe, J. D., Observation of the antiferroelectric order parameter in surface layers of $SrTiO_3$. *J. Phys. C: Solid State Phys.*, 1988, **21**, 2635–2640.
29. Weller, M., Haneczok, G. and Diehl, J., Internal-friction studies on oxygen–oxygen interaction in niobium. I. Experimental results and application of previous interpretations. *Phys. Stat. Sol. (b)*, 1992, **172**, 145–159.
30. Hünnefeld, H., Niemöller, T., Schneider, J. R., Rütt, U., Rodewald, S., Fleig, J. *et al.*, Influence of defects on the critical behavior at the 105 K structural phase transition of $SrTiO_3$: On the origin of the two length scale critical fluctuations. *Phys. Rev. B*, 2002, **66**, 14113-1-14.
31. Höchli, U. T. and Rohrer, H., Separation of the D_{4h} and O_h Phases near the Surface of $SrTiO_3$. *Phys. Rev. Lett.*, 1982, **48**, 188–191.
32. Dattagupta, S., *J. Phys. F: Metal Phys.*, 1982, **12**, 1363.
33. Dattagupta, S., Balakrishnan, R. and Ranganathan, R., Strain ordering in BCC metals and associated anelasticity. *J. Phys. F: Met. Phys.*, 1982, **12**, 1345–1362.
34. Brenscheidt, F., Seidel, D. and Wipf, H., Elastic aftereffect study of the ferroelastic tetragonal-orthorhombic phase transition in $YBa_2Cu_3O_x$. *J. Alloys Compd.*, 1994, **211/212**, 264–269.
35. Cordero, F., Ferretti, M., Cimberle, M. R. and Masini, R., Formation and mobility of oxygen vacancies in $RuSr_2GdCu_2O_8$. *Phys. Rev. B*, 2003, **67**, 144519-1-7.
36. Nowick, A. S. and Du, Y., High-temperature protonic conductors with perovskite-related structures. *Solid State Ionics*, 1995, **77**, 137–146.